# Docking and molecular dynamics studies on the interaction of four imidazoline derivatives with potassium ion channel (Kir6.2)

Rui Zhang[ab], Zhiguo Wang[ab], Baoping Ling[c], Yongjun Liu[ac]* and Chengbu Liu[c]

[a]*Northwest Institute of Plateau Biology, Chinese Academy of Sciences, Xining, Qinghai 810001, P.R. China;* [b]*Graduate University of Chinese Academy of Science, Beijing 100049, P.R. China;* [c]*School of Chemistry and Chemical Engineering, Shandong University, Jinan, Shandong 250100, P.R. China*

Kir6.2, a key component of the ATP-sensitive potassium channel ($K_{ATP}$), can directly interact with imidazoline derivatives – a kind of potential antidiabetic drug. This paper explores the interaction of Kir6.2 with four imidazoline derivatives by using AutoDock and Gromacs programs. The docking results reveal that the binding sites of the four imidazolines are different from each other: Idazoxan lies in a polar active pocket formed by residues H177, G299 and R301; while RX871024 is situated in a hydrophobic pocket composed of residues F168, M169 and I296; as for Efaroxan and Clonidine, residues H175, R177, K67 and W68 constitute the binding pocket. Based on the docking results, the four imidazoline/Kir6.2 complexes with explicit water and infinite lipid bilayer membrane were constructed to perform molecular dynamics (MD) simulation. The results of MD calculation are as follows: dioleoyl phosphatidyl choline bilayer membrane stabilised the structure of these complexes through polar and nonpolar interaction; Idazoxan and RX871024 are stably combined with Kir6.2 in their docking sites; Efaroxan has a minor change in contrast to the docking result; whereas Clonidine has an obvious change compared to docking conformation. The binding sites and interaction modes of these imidazolines with Kir6.2 may provide theoretical support in the pharmacological study of imidazoline drugs.

**Keywords:** imidazoline; $K_{ATP}$; AutoDock; Gromacs; molecular dynamics

## 1. Introduction

ATP-sensitive potassium ($K_{ATP}$) channels couple metabolism to electrical activity in many tissues by regulating $K^+$ fluxes across the cell membrane. $K_{ATP}$ channels play a multitude of functional roles in the organism, such as controlling insulin secretion from pancreatic β-cells, protecting against cardiac stress and brain seizures, mediating ischaemic preconditioning in the heart and brain, and setting the tone of vascular smooth muscle [1,2]. In glucose-sensing tissues, these channels respond to fluctuating changes in blood glucose concentration, but in other tissues they are activated only under ischaemic conditions or in response to hormonal stimulation [1].

$K_{ATP}$ channels are large hetero-octameric complexes of four pore-forming (Kir6.*x*) and four regulatory sulphonylurea receptor (SUR*x*) subunits [3]. In most tissues, Kir6.2 serves as the channel pore and SUR appears in several isoforms. As for the $K_{ATP}$ channels in pancreatic β-cells, it has a compact structure, with four SUR1 subunits embracing a central Kir6.2 tetramer in both transmembrane and cytosolic domains, as shown in Figure 1 [4]. Attempts to crystallise Kir6.2 or its C-terminal domains have proved unsuccessful. However, the crystal structures of a putative bacterial Kir channel – KirBac1.1 and the N- and C-terminal domains of its eukaryotic

counterparts – Kir3.1 have been solved [5,6]. The C domains of Kir3.1 and Kir6.2 exhibit a greater sequence identity (48%) than those of Kir6.2 and KirBac1.1 (27%), so that Haider et al. used the proximal N domain and transmembrane domains of KirBac1.1 and the distal N domain and the C domain of Kir3.1 to construct a molecular model of the Kir6.2 tetramer [7,8]. This model is consistent with a large amount of functional data and further validated by additional site-directed mutagenesis [4]. In this paper, we use the same model of Kir6.2 to identify the binding sites of imidazolines.

Imidazolines are a group of investigational antidiabetic drugs with an antihyperglycaemic but not a hypoglycaemic mode of action, because several compounds of this group enhance insulin secretion only in the presence of a stimulatory glucose concentration [9]. Studies performed over the past few years have suggested that some imidazoline derivatives may stimulate insulin secretion in a more glucose-dependent fashion than sulphonylureas [10,11]. Thus, the inherent risk of hypoglycaemias caused by the therapeutic use of sulphonylureas may be avoided. Some imidazolines blocking $K_{ATP}$ channels in pancreatic β-cells offer an explanation for their insulinotropic property [9]. Unlike sulphonylureas, which inhibit $K_{ATP}$ channel activity by binding to the regulatory subunit (SUR1) of the β-cells $K_{ATP}$ channel, imidazolines block

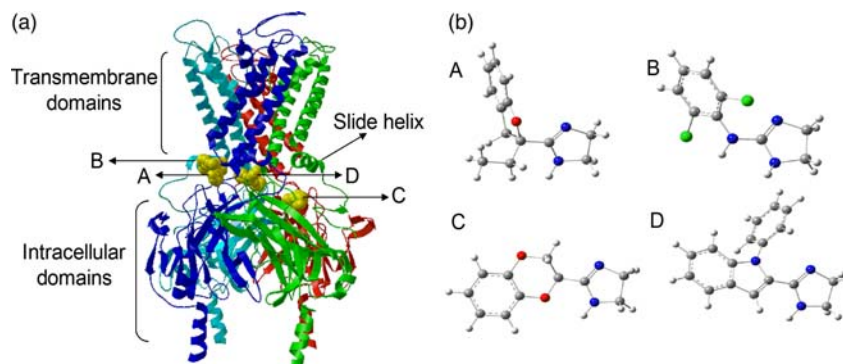Figure 1.   (a) Structures of Kir6.2 and the binding sites of imidazolines; (b) structures of imidazoline derivatives optimised at B3LYP/6-31G(d) level, (A) Efaroxan, (B) Clonidine, (C) Idazoxan, (D) RX871024.

$K_{ATP}$ channels by directly interacting with the pore-forming subunit, Kir6.2 [12,13]. However, the binding sites and the interaction details of imidazolines with Kir6.2 are still unknown. In this paper, we choose four typical imidazoline derivatives to explore the binding sites and interaction modes with Kir6.2.

The closure of the $K_{ATP}$ channel is facilitated by ATP, and its opening is potentiated by phosphoinositol (PIP2) [7,14]. Both ATP and PIP2 interact directly with Kir6.2 and the binding sites have already been determined in detail [7,14]. However, to the best of our knowledge, there is no literature that investigates the binding sites of imidazoline derivatives with Kir6.2.

In recent years, molecular docking and dynamics simulation have been widely used in studying the interaction of drugs with target proteins [15–18]. To discover how imidazoline derivatives interact with Kir6.2, we performed docking and molecular dynamics (MD) simulation based on the homology model of Kir6.2.

## 2.   Methods

There have been few studies on the interaction of drugs and ion channel, and still no theoretical research has been related to the imidazoline/Kir6.2 system. Haider et al. and Antcliffe et al. [7,14] used MD simulation and docking to investigate the binding sites of ATP and PIP2 on Kir6.2. We adopted similar methods to study the imidazolines/Kir6.2 system.

### 2.1   Ligand docking

#### 2.1.1   Structures of Kir6.2 and ligands

The structural model of Kir6.2 used in this paper is a homology model of the mouse Kir6.2 (residues 32–358; GenBank D50581) tetramer based on the X-ray crystal structures of KirBac1.1 (PDB id: 1P7B) and the intracellular domains of rat Kir3.1 (PDB id: 1N9P)

[7,14]. This model has been identified by many mutation experiments [4]. We selected four typical imidazoline derivatives widely used in pharmacological experiment, i.e. Efaroxan, Idazoxan, Clonidine and RX871024, as shown in Figure 1. Their structures were fully optimised at the level of 6-31G(d) by employing the Becke-3-parameter-Lee–Yang–Parr (B3LYP) hybrid density functional theory with Gaussian 03 package [19]. The Gasteiger–Marsili atomic charge was added to ligands and protein. It is also the selection of AutoDock while calculating the empirical free energy function.

#### 2.1.2   Docking set-up

The binding sites of imidazolines with Kir6.2 were identified by automated ligand docking using the program AutoDock v4.0 (http://www.autodock.scripps.edu/), in which the empirical free energy function and the Lamarckian genetic algorithm were employed [20,21]. All rotational bonds in ligands were set free, while the protein side chains remain fixed. At first, blind docking was applied to each ligand several times, with a grid of $216 \times 216 \times 216$ points generated with a grid spacing of 0.375 Å around the central positively charged region. After that, the dimensions of the grids were fixed on $110 \times 210 \times 210$ points around the possible binding site, also with a spacing of 0.375 Å between the grid points. This grid space defines the region of the protein in which the ligand searched for the most favourable interactions. Fifty independent docking runs were carried out for each ligand. Results were clustered according to the criterion of 1.0 Å RMSD.

### 2.2   Gromacs dynamics calculation

#### 2.2.1   Model building

Four imidazoline/Kir6.2 complexes obtained by docking were embedded in the centre of a square periodic lipid
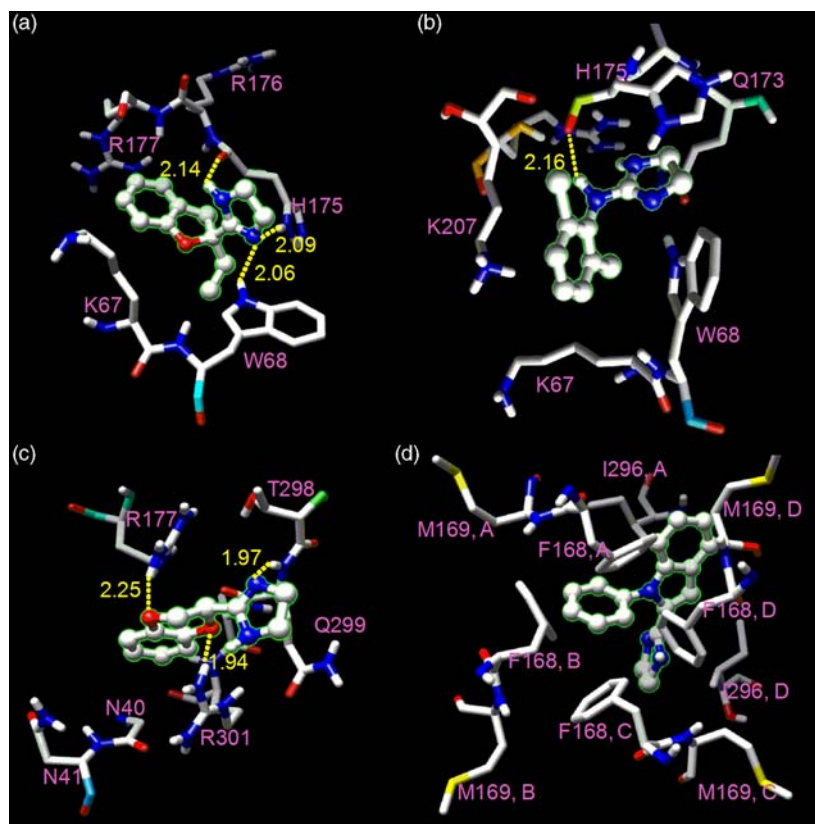
Figure 2.   Binding conformations of imidazoline derivatives derived by automated docking, only the residues within 5.0 Å are shown: (a) Efaroxan, (b) Clonidine, (c) Idazoxan, (d) RX871024. In (a)–(c), the yellow dotted lines represent the hydrogen bonds.

bilayer consisting of 340 dioleoyl phosphatidyl choline (DOPC) molecules. The overlapped DOPC molecules were deleted and 221 lipid bilayer molecules remained. The resulting systems were solvated with ~120,000 SPC waters and then neutralised by counter ions at random positions. This generated a system of ~406,880 atoms.

### 2.2.2   *Gromacs dynamics set-up*

MD simulations of the imidazoline/Kir6.2 systems were carried out with Gromacs-3.3.1-1 suite of programs with the Gromacs force field (http://www.gromacs.org) [22]. We used the PRODRG2 server to parameterise the four imidazoline drugs [23]. All of the complexes were first energy minimised with the steepest descent method; then a 200 ps position restraining simulation was carried out restraining the Kir6.2 by a 1000 kJ/mol Å$^2$ harmonic constraint to relieve close contacts before the actual simulation; finally, a 3 ns MD simulation was performed. We applied the leap-frog algorithm in the NPT ensemble, and each component, imidazoline, Kir6.2, DOPC, H$_2$O and Na$^+$ was separately coupled. The Berendsen temperature coupling and Berendsen pressure coupling

(the coupling constants were both set to 0.1) were used to keep the system in a stable environment (300 K, 1 Bar). During these steps, the particle mesh Ewald (PME) method for long-range electrostatics, a 10 Å cut-off for van der Waals interactions, a 9 Å cut-off for Coulomb interaction and the LINCS algorithm for bond constraints were used [24,25].

## 3.   Results and discussion

### 3.1   *Docking*

#### 3.1.1   *Binding sites*

The left side of Figure 1 shows the binding sites of the four imidazoline derivatives. Each ligand corresponds to different locations on the Kir6.2 subunit. For clarity, only one binding site of each drug is shown, because the location of the same drug on the four monomers of Kir6.2 is identical. Though the binding sites are different, the locations of each drug on the same monomer are close to each other. Efaroxan and Clonidine lie near to the slide helix of C-terminal, and their binding sites are partially overlapped. The binding site of Idazoxan is located in the intracellular domains, while RX871024 lies in the centre of the channel pore, directly blocking the channel.

Table 1. Binding and docking energies of imidazolines and Kir6.2 calculated by AutoDock4.0.

| Imidazolines | Binding energy (kcal/mol) | Docking energy (kcal/mol) | Inhibition constant (μM; 298.15 K) |
| --- | --- | --- | --- |
| Idazoxan | − 6.62 | − 7.13 | 13.91 |
| Efaroxan | − 6.40 | − 6.91 | 19.07 |
| Clonidine | − 4.95 | − 5.25 | 234.01 |
| RX871024 | − 6.58 | − 7.83 | 15.06 |

Figure 2 shows the residues that directly interact with these ligands. As shown in Figure 2(a),(b), Efaroxan forms two hydrogen bonds with H175 and one hydrogen bond with W68, with bond lengths of 2.09, 2.14 and 2.06 Å, respectively; Clonidine forms only one hydrogen bond with H175 with a bond length of 2.16 Å. Figure 2(c) displays the binding site of Idazoxan, which is located in the intracellular domains. Idazoxan forms three hydrogen bonds with R177, Q299 and R301, and the bond length is 2.25, 1.97 and 1.94 Å, respectively. Unlike the other ligands, RX871024 is located in the pore of the Kir6.2 channel. From Figure 2(d), we can see that all the four monomers of Kir6.2 interact with RX871024, the residues F168, M169 and I296 are all hydrophobic, and no hydrogen bonds are formed.

The AutoDock program also calculates the binding and docking energies. The energy items include intermolecular energy (constituted by van der Waals energy, hydrogen bonding energy, desolvation energy and electrostatic energy), internal energy and torsional energy. The first two items build up docking energy, the first and the third items compose the binding energy. Table 1 shows the energy information of the four ligands. Clonidine corresponds to the lower binding energy ($-4.95$ kcal/mol), while the other ligands correspond to the higher values ($\sim -6.5$ kcal/mol). The docking energies show the same tendency as the binding energy. Inhibition constant was also calculated with the order of Clonidine $\gg$ Efaroxan $\approx$ RX871024 $\approx$ Idazoxan.

Figure 3 shows the lipophilic potential surfaces of residues within 6.0 Å around the ligands. As the colour changes from blue to red, the surface transforms from hydrophilic to hydrophobic. Figure 3(a) shows the surface of Efaroxan, which is located in a hydrophilic surface; Figure 3(b) is the lipophilic potential surface of Clonidine, the hydrophilicity of the surface is weaker than Efaroxan
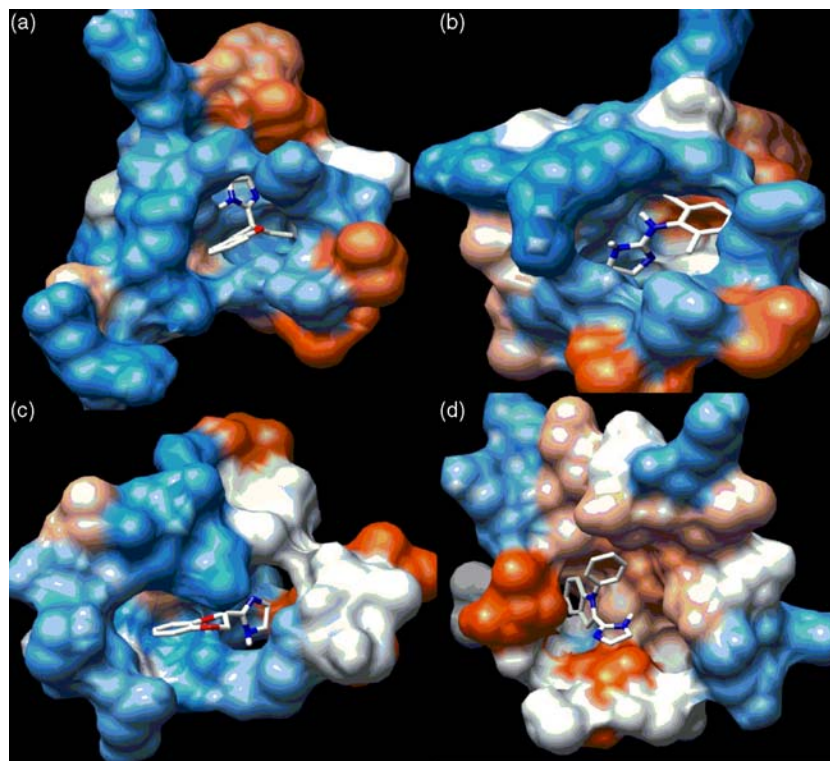


Figure 3. Lipophilic potential surface of the surrounded residues within 6.0 Å. As the colour changes from blue to red, the surface changes from hydrophilic to hydrophobic. (a) Efaroxan, (b) Clonidine, (c) Idazoxan, (d) RX871024.
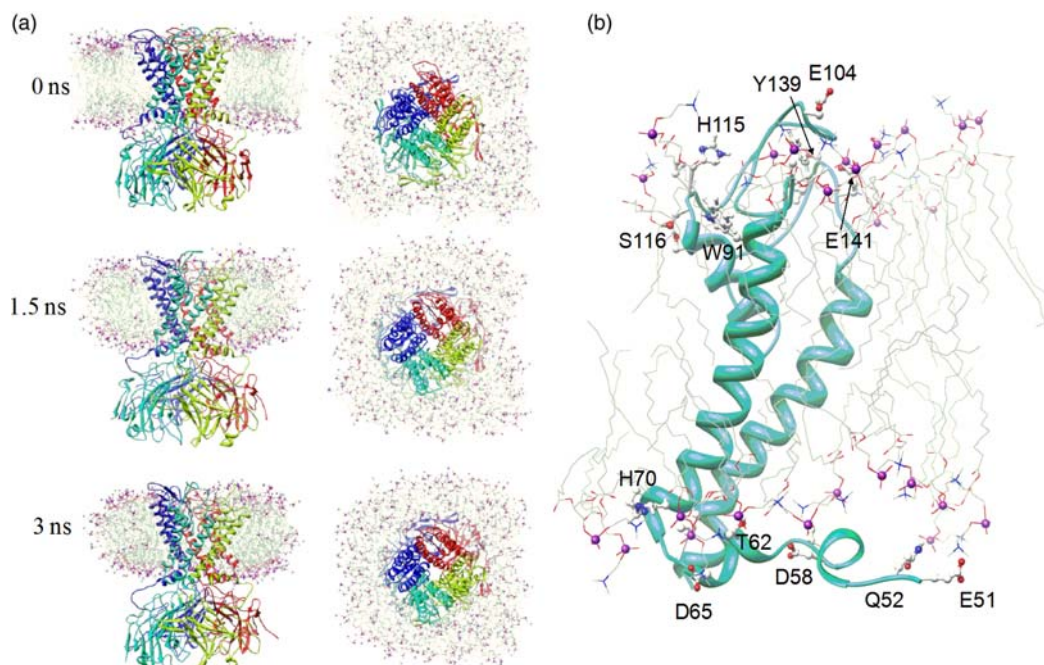
Figure 4.    (a) The side and top view of the Kir6.2 in DOPC membrane of MD simulation in 0, 1.5 and 3 ns; (b) the interaction between transmembrane region of one monomer and DOPC molecules within 5 Å. We deleted the last 27 residues of each monomer in Kir6.2 which are far away from the ligand binding site and the transmembrane region to reduce the volume of these systems.

and is more prone to hydrophobic; from Figure 3(c), it can be seen that the surface around Idazoxan is almost completely hydrophilic; while in Figure 3(d), all residues around RX871024 are hydrophobic. These results are in accordance with the intrinsic character of the four imidazolines.

From the docking results, four different binding sites were obtained, which were closely related to the structures of these drugs. The experiments did not gain the binding sites about imidazolines with Kir6.2, but the docking provided us with the possible binding sites.

### 3.1.2   Comparison of the binding sites with PIP2

Haider et al. [14] have already studied the binding site of PIP2 with Kir6.2 in detail. The PIP2 molecule can extend up to $\sim 17$ Å on the binding site and directly interact with many residues, including R176, R177, E179, Q299 and R301 at C-terminals, K39 and N41 at N-terminals, and K67 at transmembrane domains [14]. Among the four imidazolines, the binding site of Idazoxan is most similar to that of PIP2. Idazoxan interacts with Kir6.2 by forming three hydrogen bonds with R177, Q299 and R301 and strong van der Waals interaction with R176 and N41 in the binding pocket.

The binding sites of Efaroxan and Clonidine are different from those of Idazoxan but still near to those of PIP2. Some residues like R176, R177 and K67 are in the binding site of PIP2 and the two imidazolines. There are no hydrogen bonds between these two imidazolines and the pocket residues; therefore, the main interaction is nonpolar interaction.

Different from other three imidazolines and PIP2, RX871024 is located in the channel pore of Kir6.2 due to its appropriate size and hydrophobicity. From Figure 2(d), we can see that the interactional residues including F168, A172 and I296 are all hydrophobic and no hydrogen bonds were formed. It is the hydrophobic interaction that makes RX871024 lie in the channel pore of Kir6.2 and directly block the channel.

### 3.1.3   The relationship of the function and binding mode

The function of drugs is closely related to their binding sites and interaction mode. Experiments have revealed that imidazolines are potential inhibitors of $K_{ATP}$ channel. RX871024 exhibits an inhibition of 82% at the concentration of $10\,\mu$M [26]; while Efaroxan achieves the same inhibition at the concentration of $100\,\mu$M [26]. Idazoxan is the weakest inhibitor among the four imidazolines; its inhibition is lower than 50% even at its maximal concentration. Clonidine, as $K_{ATP}$ inhibitor, shows moderate activity between that of Efaroxan and Idazoxan. Therefore, the order of the inhibitory activity
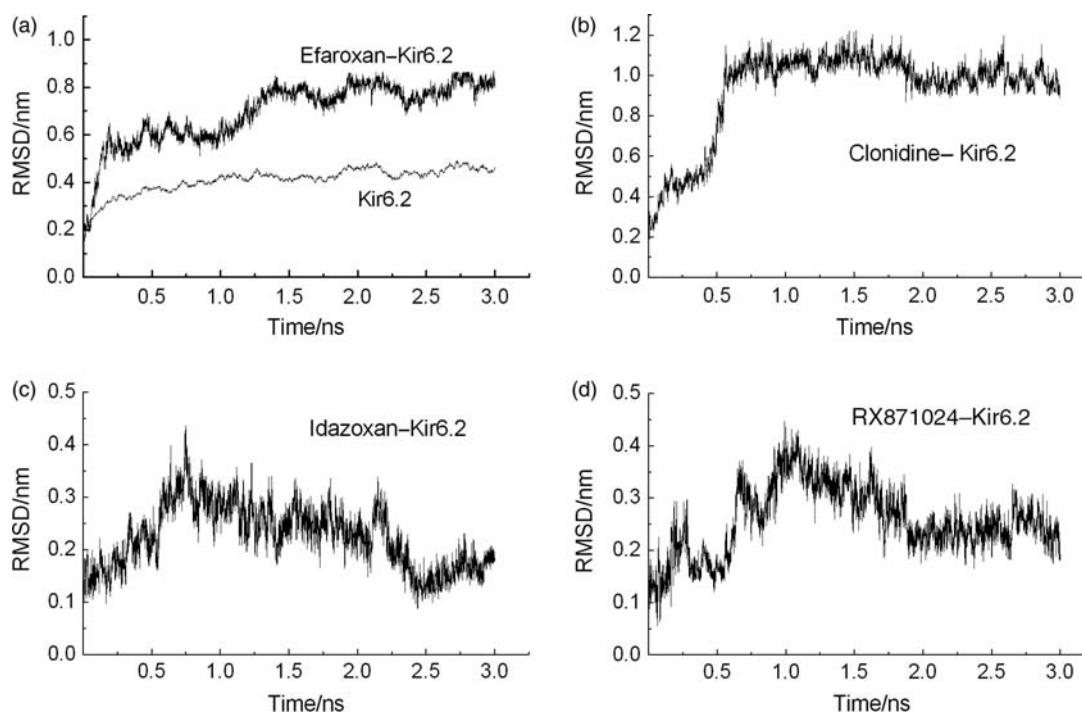
Figure 5.  RMSDs of imidazolines relative to Kir6.2 derived by molecular dynamic calculation using Gromacs software. The RMSD of Kir6.2 relative to itself is also presented in the red curves in Figure 4(a).

is RX871024 > Efaroxan > Clonidine > Idazoxan [26,27]. We can explain their inhibitory activity by checking their binding sites. RX871024 is located in the channel pore which is the most active position to inhibit the $K_{ATP}$; while the binding site of Idazoxan is far away from the channel pore which is the weakest position; Efaroxan and Clonidine have moderate inhibiting activity on their binding sites which are near to the channel pore.

Imidazolines also stimulate the secretion of insulin, which is mediated by the blockade of Kir6.2. The order of the activity is RX871024 > Efaroxan > Clonidine $\gg$ Idazoxan [28,29]. Idazoxan works only at very high concentration. Comparing Efaroxan with RX871024, the latter shows a lower activity at low glucose concentration in stimulating the secretion of insulin, but exhibits a higher activity at high glucose concentration; so RX871024 shows higher potential as an antidiabetic drug [28,29]. The order of the four imidazolines in stimulating the secretion of insulin and the inhibitory activity of $K_{ATP}$ channel is the same. So we can deduce that the stimulation of insulin secretion is also closely related to the inhibitory activity and the binding sites.

Imidazolines have been studied for the purpose of treating type-1 and type-2 diabetes. In recent years, there have been many new imidazoline medicines investigated, such as BL11282 and NNC77-0074 [30,31]. But not all imidazolines can be used to treat diabetes because of the β-cell toxicity. The toxicity is due to individual properties of the imidazolines and is different from the sequence of the $K_{ATP}$ channel-blocking and insulin-releasing effect; Efaroxan has no β-cell toxicity, Idazoxan is markedly β-cell toxic and RX871024 has a mediated toxicity [32,33]. The relationship of toxicity and the binding sites of imidazolines on Kir6.2 is still unclear and further studies are required.

### 3.2  Molecular dynamics simulation

#### 3.2.1  Interaction of DOPC with Kir6.2

Each system for MD simulation contains Kir6.2, ligand, DOPC, $Na^+$ and $H_2O$. DOPC molecules, as a lipid bilayer membrane, were arranged around the Kir6.2 tetramer. After 1 ns of MD calculation and afterwards, Kir6.2 was tightly surrounded by DOPC molecules through polar and nonpolar interactions, as shown in Figure 4(a). The detailed interaction after 3 ns of MD simulation between Kir6.2 and DOPC molecules within 6 Å is displayed in the right panel in Figure 4(b). For clarity, only the transmembrane region of one monomer of Kir6.2 is shown. The important residues which have polar interaction with DOPC are pointed out. In these systems, though the binding sites of these ligands are far away from the transmembrane region, the lipid bilayer membrane prevented the arbitrary movement between the four monomers of Kir6.2, and they play an important role in stabilising these systems.

### 3.2.2    *Stability of the ligand/Kir6.2 systems*

Based on the docking results, MD simulations on the four drug/protein complexes (Idazoxan–Kir6.2, Efaroxan–Kir6.2, Clonidine–Kir6.2 and RX871024–Kir6.2) were carried out by Gromacs program. We examined the stability of Kir6.2 by a 3 ns MD simulation and the following RMSD calculation. Results show that Kir6.2 becomes equilibrated at 1 ns and afterwards, which is in accordance with the results of Haider et al. [14]. Then, the RMSDs of imidazolines relative to Kir6.2 and of protein relative to protein were obtained based on the MD simulation of all the systems to get the information of positional fluctuations, as shown in Figure 5. From the curve of Figure 5(a), we can see that Kir6.2 was stabilised by DOPC and the RMSD value of protein relative to protein is about 0.4 nm.

From Figure 5(a), it can be seen that Efaroxan seems stabilised relative to Kir6.2 at 1.5 ns judging by its RMSD value ($\sim$ 0.85 nm). By checking the interval conformations, we noticed small changes in the binding mode. All the original hydrogen bonds vanished and were substituted by new ones. For example, Efaroxan and D65 formed one or two new hydrogen bonds which locate in the polar hydrogen of imidazoline ring and carbonyl O in D65.

From Figure 5(b), we can see that Clonidine has a smooth RMSD curve after 1 ns of simulation and the average RMSD value is 1.05 nm. At the first 0.7 ns, the RMSD curve has a sharp rise and then becomes smooth. When checking the interval conformations, we find that the conformation of Clonidine has changed a lot after 0.7 ns. Though the active pocket is also near the original pocket, new residues interacting with Clonidine are observed (for example I162 and T171). The original

hydrogen bond also disappeared at 0.7 ns, and no new hydrogen bond formed.

Figure 5(c) is the RMSD of Idazoxan, the stable conformation formed after 1 ns with the average RMSD value of about 0.25 nm. When examining the interval conformations, it can be seen that at 1 ns the conformation changes a little, then at 1.3 ns, the conformation returns to the original conformation and afterwards. The hydrogen bonds changed a little: one of these on R301 keeps stable in the time of dynamics simulation; other hydrogen bonds changed and were replaced by new ones. The new hydrogen bond forms between the polar hydrogen of imidazoline ring and carbonyl O in E292.

Figure 4(d) shows the RMSD of RX871024; because it is located in the channel pore, the conformation is difficult to change with RMSD value of $\sim$ 0.25 nm. Just like Idazoxan, the conformation of RX871024 changed a little at the first 1 ns; then it came back to the original conformation. That is to say RX871024 is stably bonded to Kir6.2 on its binding site.

From the RMSDs and interval conformations of imidazolines, we can see that the dynamic simulation is in accordance with the docking results except a visible conformation change in Clonidine. The possible reason is that Clonidine has the lowest docking energy, and the conformation change in dynamic simulation may reach the lower energy domain. In addition we gained the average structure of Kir6.2 and ligands by MD simulation (see Figure 6). From the binding site of ligands and the surface of surrounding residues we can see that all the ligands were in proper position with correspondingly stable binding and had little change compared to the docking result.
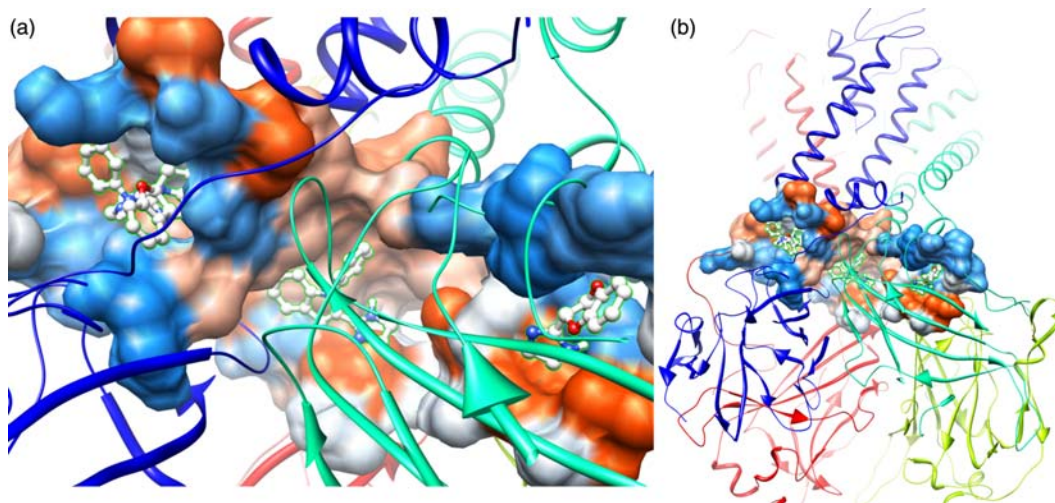


Figure 6.    Focus-view (a) and side-view (b) of the surface around the ligands derived from the average structure of 3ns MD simulation. As the colour changes from green to red, the surface changes from hydrophobic to hydrophilic; Kir6.2 is shown in ribbons and each monomer of it is in a different colour; Ligands are in ball and stick form.

## 4. Conclusion

We applied docking and MD simulation to study the binding sites of imidazolines on Kir6.2 channel. Four imidazolines have different binding sites and interaction modes on Kir6.2. From these results, we can see that hydrogen bond and hydrophobic interaction contribute to the stable binding. The dynamic simulation is in accordance with the docking results except a visible conformational change in Clonidine, and the reason lies in the unstable binding of Clonidine with a lower binding energy on Kir6.2. The function and binding sites have a close relationship according to the results of docking and experiments.

## Acknowledgements

## References

[1] S. Seino and T. Miki, *Physiological and pathophysiological roles of ATP-sensitive K$^+$ channels*, Prog. Biophys. Mol. Biol. 81 (2003), pp. 133–176.

[2] C.G. Nichols, *K$_{ATP}$ channels as molecular sensors of cellular metabolism*, Nature 440 (2006), pp. 470–476.

[3] M.V. Mikhailov, J.D. Campbell, H. De Wet, K. Shimomura, B. Zadek, R.F. Collins, M.S.P. Sansom, R.C. Ford, and F.M. Ashcroft, *3-D structural and functional characterization of the purified K$_{ATP}$ channel complex Kir6.2–SUR1*, EMBO J. 24 (2005), pp. 4166–4175.

[4] S. Haider, J.F. Antcliff, P. Proks, M.S.P. Sansom, and F.M. Ashcroft, *Focus on Kir6.2: a key component of the ATP-sensitive potassium channel*, J. Mol. Cell. Cardiol. 38 (2005), pp. 927–936.

[5] A. Kuo, J.M. Gulbis, J.F. Antcliff, T. Rahman, E.D. Lowe, J. Zimmer, J. Cuthbertson, F.M. Ashcroft, T. Ezaki, and D.A. Doyle, *Crystal structure of the potassium channel KirBacl.l in the closed state*, Science 300 (2003), pp. 1922–1926.

[6] M. Nishida and R. Mackinnon, *Structural basis of inward rectification: cytoplasmic pore of the G protein-gated inward rectifier GIRK1 at 1.8 Å resolution*, Cell 111 (2002), pp. 957–965.

[7] J.F. Antcliff, S. Haider, P. Proks, M.S.P. Sansom, and F.M. Ashcroft, *Functional analysis of a structural model of the ATP-binding site of the K$_{ATP}$ channel Kir6.2 subunit*, EMBO J. 24 (2005), pp. 229–239.

[8] S. Trapp, S. Haider, P. Jones, M.S.P. Sansom, and F.M. Ashcroft, *Identification of residues contributing to the ATP-binding site of Kir6.2*, EMBO J. 22 (2003), pp. 2903–2912.

[9] A. Wienbergen, C. Bleck, T.G. Lackmann, and I. Rustenbeck, *Antagonism of the insulinotropic action of first generation imidazolines by openers of K$_{ATP}$ channels*, Biochem. Pharmacol. 73 (2007), pp. 94–102.

[10] A. Takahashi, K. Nagashima, A. Hamasaki, N. Kuwamura, Y. Kawasaki, H. Ikeda, Y. Yamada, N. Inagaki, and Y. Seino, *Sulfonylurea and glinide reduce insulin content, functional expression of K$_{ATP}$ channels, and accelerate apoptotic β-cell death in the chronic phase*, Diabetes Res. Clin. Pract. 77 (2007), pp. 343–350.

[11] I. Rustenbeck, C. Herrmann, P. Ratzka, and A. Hasselblatt, *Imidazoline/guanidinium binding sites and their relation to inhibition of KATP channels in pancreatic B-cells*, Naunyn-Schmiedeberg's Arch. Pharmacol. 356 (1997), pp. 410–417.

[12] P. Proks and F.M. Ashcroft, *Phentolamine block of K$_{ATP}$ channels is mediated by Kir6.2*, Proc. Natl Acad. Sci. 94 (1997), pp. 11716–11720.

[13] G.T. Lackmann, B.J. Zűnkler, and I. Rustenbeck, *Specificity of non-adrenergic imidazoline binding sites in insulinsecreting cells and relation to the block of ATP-sensitive K$^+$ channels*, Ann. N. Acad. Sci. 1009 (2003), pp. 371–377.

[14] S. Haider, A.I. Tarasov, T.J. Craig, M.S.P. Sansom, and F.M. Ashcroft, *Identification of the PIP2-binding site on Kir6.2 by molecular modelling and functional analysis*, EMBO J. 26 (2007), pp. 3749–3759.

[15] N.S. Kang, C.H. Chae, and S.-E. Yoo, *Study on the hydrolysis mechanism of phosphodiesterase 4 using molecular dynamics simulations*, Mol. Simul. 32 (2006), pp. 369–374.

[16] I. Ryuichiro, T. Tohru, and S. Kentaro, *Refinement of comparative models of protein structure by using multicanonical molecular dynamic simulation*, Mol. Simul. 34 (2008), pp. 327–336.

[17] Y. Mine, *Molecular dynamic simulation of model lipid membranes: structural effects of impurities*, Mol. Simul. 27 (2001), pp. 187–197.

[18] N. Takashi, T. Hiromi, and H. Yoshimichi, *Interaction between a twelve-residue segment of antifreeze protein type I, or its mutants, and water molecules*, Mol. Simul. 34 (2008), pp. 309–325.

[19] M.J. Frisch, G.W. Trucks, H.B. Schlegel, G.E. Scuseria, M.A. Robb, J.R. Cheeseman, J.A. Montgomery, Jr., T. Vreven, Jr, K.N. Kudin, J.C. Burant, J.M. Millam, S.S. Iyengar, J. Tomasi, V. Barone, B. Mennucci, M. Cossi, G. Scalmani, N. Rega, G.A. Petersson, H. Nakatsuji, M. Hada, M. Ehara, K. Toyota, R. Fukuda, J. Hasegawa, M. Ishida, T. Nakajima, Y. Honda, O. Kitao, H. Nakai, M. Klene, X. Li, J.E. Knox, H.P. Hratchian, J.B. Cross, C. Adamo, J. Jaramillo, R. Gomperts, R.E. Stratmann, O. Yazyev, A.J. Austin, R. Cammi, C. Pomelli, J.W. Ochterski, P.Y. Ayala, K. Morokuma, G.A. Voth, P. Salvador, J.J. Dannenberg, V.G. Zakrzewski, S. Dapprich, A.D. Daniels, M.C. Strain, O. Farkas, D.K. Malick, A.D. Rabuck, K. Raghavachari, J.B. Foresman, J.V. Ortiz, Q. Cui, A.G. Baboul, S. Clifford, J. Cioslowski, B.B. Stefanov, G. Liu, A. Liashenko, P. Piskorz, I. Komaromi, R.L. Martin, D.J. Fox, T. Keith, M.A. Al-Laham, C.Y. Peng, A. Nanayakkara, M. Challacombe, P.M.W. Gill, B. Johnson, W. Chen, M.W. Wong, C. Gonzalez, and J.A. Pople, Gaussian 03, Revision C.02, Gaussian, Inc., Wallingford, CT (2004).

[20] G.M. Morris, D.S. Goodsell, R.S. Halliday, R. Huey, W.E. Hart, R.K. Belew, and A.J. Olson, *Automated docking using a Lamarckian genetic algorithm and empirical binding free energy function*, J. Comput. Chem. 19 (1998), pp. 1639–1662.

[21] M.F. Sanner, *Python: A programming language for software integration and development*, J. Mol. Graph. Model 17 (1999), pp. 57–61.

[22] E. Lindahl, B. Hess, and D. Van Der Spoel, *GROMACS 3.0: a package for molecular stimulation and trajectory analysis*, J. Mol. Model 7 (2001), pp. 306–317.

[23] A.W. Schuettelkopf and D.M.F. Van Aalten, *PRODRG - a tool for high-throughput crystallography of protein-ligand complexes*, Acta. Cryst. D 60 (2004), pp. 1355–1363.

[24] T. Darden, D. York, and L.J. Pedersen, *Particle mesh Ewald—an N.log(N) method for Ewald sums in large systems*, J. Chem. Phys. 98 (1993), pp. 10089–10092.

[25] B. Hess, H. Bekker, H.J.C. Berendsen, and J.G.E.M. Fraaije, *LINCS: a linear constraint solver for molecular simulations*, J. Comput. Chem. 18 (1997), pp. 1463–1472.

[26] M. Willenborg, A. Wienbergen, L. Aguilar-Bryan, J. Bryan, and I. Rustenbeck, *RX871024 but not Efaroxan stimulates insulin secretion by a K$_{ATP}$ independent mechanism*, Diabetologie und Stoffwechsel S1 (2007), Freie Vorträge 6 – Insulinsekretion, V50.

[27] H. Gao, M. Mourtada, and N.G. Morgan, *Effects of the imidazoline binding site ligands, idazoxan and efaroxan, on the viability of insulin-secreting BRIN-BD11 cells*, J. Pancreas 4 (2003), pp. 117–124.

[28] M. Mourtada, S.A. Smith, and N.G. Morgan, *Effector systems involved in the insulin secretory responses to efaroxan and RX871024 in rat islets of Langerhans*, Eur. J. Pharmacol. 350 (1998), pp. 251–258.

[29] M. Mourtada, S.L.F. Chan, S.A. Smith, and N.G. Morga, *Multiple effector pathways regulate the insulin secretory response to the imidazoline RX871024 in isolated rat pancreatic islets*, Br. J. Pharmacol. 127 (1999), pp. 1279–1287.

[30] A.M. Efanov, S.V. Zaitsev, M. Hans-Juergen, A. Raap, I.B. Appelskog, O. Larsson, B. Per-Olof, and S. Efendic, *The novel imidazoline compound BL11282 potentiates glucose-induced insulin secretion in pancreatic b-cells in the absence of modulation of $K_{ATP}$ channel activity*, Diabetes 50 (2001), pp. 797–802.

[31] M. Høy, H.L. Olsen, H.S. Andersena, K. Bokvist, K. Buschard, J. Hansen, P. Jacobsen, J.S. Petersen, P. Rorsman, and J. Gromada, *Imidazoline NNC77-0074 stimulates insulin secretion and inhibits glucagon release by control of $Ca^{2+}$-dependent exocytosis*

*in pancreatic a- and β-cells*, Eur. J. Pharmacol. 466 (2003), pp. 213–221.

[32] I. Rustenbeck, A. Krautheim, A. Jörns, and H.J. Steinfelder, *β-Cell toxicity of ATP-sensitive $K^+$ channel-blocking insulin Secretagogues*, Biochem. Pharmacol. 67 (2004), pp. 1733–1741.

[33] I.I. Zaitseva, J. Størling, T. Mandrup-Poulsen, P.O. Berggren, and S.V. Zaitsev, *The imidazoline RX871024 induces death of proliferating insulin-secreting cells by activation of c-jun N-terminal kinase*, Cell. Mol. Life Sci. 65 (2008), pp. 1248–1255.